Retraction

Retracted: Computer 3D Scene Simulation of Ecological Landscape Layout Planning

Advances in Multimedia

This article has been retracted by Hindawi following an investigation undertaken by the publisher [1]. This investigation has uncovered evidence of one or more of the following indicators of systematic manipulation of the publication process:

(1) Discrepancies in scope

(2) Discrepancies in the description of the research reported

(3) Discrepancies between the availability of data and the research described

(4) Inappropriate citations

(5) Incoherent, meaningless and/or irrelevant content included in the article

(6) Peer-review manipulation

The presence of these indicators undermines our confidence in the integrity of the article's content and we cannot, therefore, vouch for its reliability. Please note that this notice is intended solely to alert readers that the content of this article is unreliable. We have not investigated whether authors were aware of or involved in the systematic manipulation of the publication process.

Wiley and Hindawi regrets that the usual quality checks did not identify these issues before publication and have since put additional measures in place to safeguard research integrity.

We wish to credit our own Research Integrity and Research Publishing teams and anonymous and named external researchers and research integrity experts for contributing to this investigation.

The corresponding author, as the representative of all authors, has been given the opportunity to register their agreement or disagreement to this retraction. We have kept a record of any response received.

References

[1] T. Ling and Y. Ma, "Computer 3D Scene Simulation of Ecological Landscape Layout Planning," *Advances in Multimedia*, vol. 2022, Article ID 6602095, 11 pages, 2022.

Hindawi

Research Article

Computer 3D Scene Simulation of Ecological Landscape Layout Planning

Tong Ling and Yun Ma [ID]

Apparel Art Design College, Xi'an Polytechnic University, Xi'an, China

Correspondence should be addressed to Yun Ma; 210311022@stu.xpu.edu.cn

There are some problems in traditional 3D landscape construction and virtual display, such as inflexible landscape spatial organization and limitations of virtual garden simulation in reality. Virtual reality, virtual plants and geographic information systems, and other technologies are used. Based on parameterized method in constructing 3D landscape scene, the main elements of the landscape were, respectively, constructed and rendered in 3D model, and a complete 3D landscape scene construction model was formed. OpenGL shader language was used for rendering, improved NSGA-II algorithm was used with the help of bionic logic of the genetic evolution process to achieve landscape land allocation optimization. The experimental result shows: through 3D scene view clipping hierarchical detail model and other techniques, the frame rate of 3D landscape vegetation scene drawing was improved. The interactive 3D scene browsing is realized, and the six-degree-of-freedom omni-directional display of the whole landscape is provided.

1. Introduction

Landscape architecture is an applied discipline based on natural science and humanities. With the improvement of living standards and the change in environmental conditions, people's ecological concepts being strengthened, the field of landscape design is gradually expanding, and the public's participation is improved [1]. There are many problems in landscape design: valuing part over whole, valuing effect over reality, feeling over reason, and experiencing over science. The lack of relevant professional software, display analysis, and evaluation function seriously hinders the development of modern landscape. People gradually try to introduce visual digital technology into landscape design and make it become a breakthrough in the development of future landscapes. With the development of information technology, computer technology is more and more widely used in the process of landscape design. 3D visualization digital technology is a new force of computer technology, 3D visualization digital technology has been in many application fields, and gradually popularized because

it is good at management, analysis and prediction, and other functions. At present, 3D visualization technology has also begun to be widely used in landscape design and expression, expanding the new field of landscape design [2, 3]. However, the application research in the landscape is still immature, and there are few practical applications of more effective technologies in the expression of landscape design schemes, so it is necessary to further explore and excavate its advantages and connotations. Therefore, using the advantages of 3D visualization digital technology in the auxiliary aspect, explore and excavate its practical operation technology in the expression of landscape design scheme so that 3D visualization digital technology can participate in the process of landscape design scheme expression. Figure 1 shows the simulation system design of landscape planning effect based on virtual reality technology.

2. Literature Review

The word landscape appears in earlier descriptions of the landscape of Jerusalem, and over time it has been expressed

The user layer
Landform, vegetation cover,
climate, sound, rivers and lakes,
architecture, etc
Lidar, GPS, sensors

The application layer
Main control device/
AVR microcontroller

According to layer
Output devices
Projector, stereo display system,
stereo earphone,
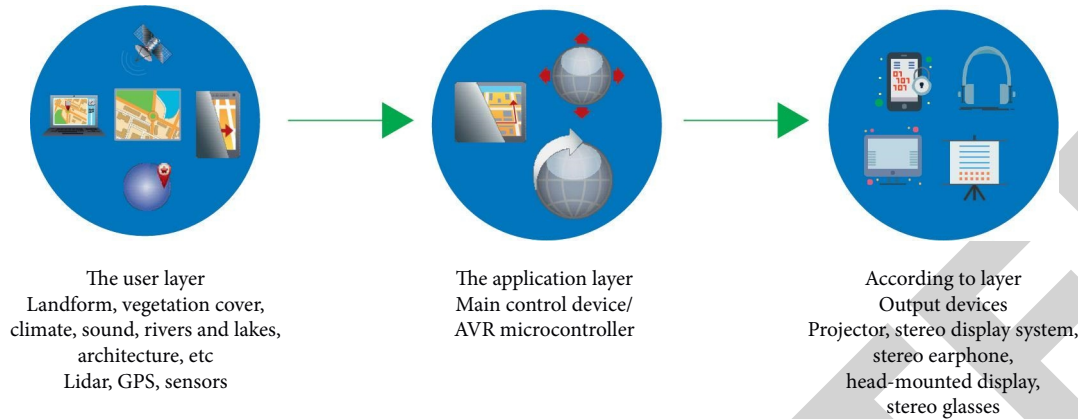head-mounted display,
stereo glasses

FIGURE 1: Design of simulation system of landscape planning effect based on virtual reality technology.

and interpreted differently in different disciplines. In geography, ecology, and landscape science, it has its own disciplinary expression. For example, in geography, landscape is regarded as a natural complex with uniform integrity and diversity. Landscape in a broad sense not only refers to a certain area or some form of natural scenery but also includes man-made landscape. Before the invention of visualization technology, landscape effects were generally presented by hand-painted photos or film records. With the development of the times and the progress of science and technology, visualization technology is an important means to show landscape effects. Landscape visualization is mainly in the visualization technology, the data in the landscape are analyzed and sorted out, it is displayed to the user, and the landscape management can be carried out, and finally, realize the visualization of the landscape.

In recent years, the rapid development of image processing computer-level geographic information systems, virtual reality and artificial intelligence provide a broad platform for the research and application of landscape visualization. In an international symposium named OurVisual Scape, the research of landscape visualization has been aroused once again. More and more scholars at home and abroad focus on the development and application of landscape modeling and computer graphics, such as the application of visualization technology in vegetation landscape modeling, urban management, and garden design plant planting. At the same time, there are some people mainly for landscape simulation and visualization tools and other aspects of the research with the development of society, the progress of science and technology, landscape visualization, and the development of landscape visualization into the three-dimensional landscape visualization stage [4].

Compared with the two-dimensional landscape visualization stage, the development of software and hardware technology in this stage is relatively more rapid. In terms of computer, its operation speed has exceeded one billion times, and the graphics display card can also carry out better data operation and processing so that the landscape visualization is more real. Landscape visualization equipment has also been developed and produced, such as stereo projection system, digital helmet, digital glove, and ball screen display system. Along with this comes a series of 3D landscape visualization software (like UTOOLS and UVIEW, persistence of vision raytracer (POV-Ray), VistaPro3, gnu image manipulation program (GIMP), smart forest, landscape management system (LMS), (VisuaIFX, VisualExplorer, TruFIite, CLRview, CCGIS, etc.) [5, 6].

The main characteristics of the 3D landscape visualization stage are as follows: the 3D model of individual landscapes such as buildings and vegetation are established, the 3D landscape graphics and images superimposed by entities are used to represent the landscape content, and the dynamic interaction of data in each part is used to represent the landscape changes. The landscape visualization in this period has realized the perfect transformation from landscape representation to landscape simulation, from a static display to interactive and simulation, from two-dimensional plane graphics to three-dimensional solid model. People not only begin to pay attention to the visualization of crops but also pay more and more attention to the influence of plant visualization in landscape design, so as to build a better communication bridge between professional designers and the public. Research on visualization and computer simulation of plant growth, University of Calgary, Canada, on fractal generators of plants. Through field observation and measurement, the change parameters of various parts of organs and morphological structure in the process of plant growth are obtained, and then the simulation of plant growth is carried out by computer. The dynamic visualization of plants is to change the growth and change process of plants from two-dimensional to three-dimensional or even four-dimensional after the simulation of plant growth is realized in the calculation so that the growth of plants can be dynamically displayed over time [7].

3. 3D Landscape Construction and Accelerated Rendering

Three-dimensional construction of landscape scenes, according to the composition of different actual gardens, need to build different landscape tree model building model three-dimensional terrain. Taking into account the realistic elements of gardens, such as water reflection weather factors

scene occlusion. Finally, the whole realistic 3D landscape is formed. Develop 3D landscape virtual display system, provide landscape scene virtual display platform, and meet the realistic requirements of landscape virtual experience. It also provides a multi-angle means of evaluation, appreciation, and browsing for the constructed 3D landscape scene. This chapter describes the virtual display process of three-dimensional landscape construction through the three-dimensional landscape construction of parametric spatial organization of landscape and acceleration of scene vegetation rendering [8].

3.1. 3D Landscape Sense Creation

3.1.1. 3D Geometric Tree Model Construction Process. In the parametric tree 3D model construction, firstly, it is necessary to collect the appearance data of various tree structures in the corresponding garden area and conduct the corresponding appearance modeling of tree structures according to the parametric data. Taking the common ornamental tree frangipani yellow in the experimental area of this paper as an example, specific trees can be interpreted as the following parameterized data Table 1 [9].

Table 1 specifically divided the structure of *Fritillaria japonicum* into four branches including the main branch. The overall morphological structure of *Fritillaria japonicum* was described through data such as the length of branches at different levels, internode length of branches, and branch angle. Due to a large number of final branches (tertiary branches), they are usually built in batches by automatic generation in parametric modeling software, and then optimized and adjusted the crown shape of tree morphological structure according to field photos; The leaf density in the table ultimately determines the number of leaves in the three-dimensional tree model, and its numerical value is the ratio of the total number of leaves to the spatial volume of tree crown (the corresponding cylinder volume formed by crown width and crown height) [10, 11].

The specific construction process is shown in Figure 2. Based on OpenGL graphics standard, ParaTree builds a tree model through tree rendering engine. Firstly, it provides users with template basis by generating default tree model; then, according to user-defined attribute data, such as trunk DBH or whorl texture parameters, branch angle, leaf form, and leaf density, the tree was redrawn based on the tree template; finally, a parameterized tree model with high sense of reality is generated by setting global parameters, such as LOD illumination material, and exported [12].

3.1.2. Tree Visualization Process. The 3D geometric tree model constructed by parametric modeling method has a complete branch and leaf hierarchy structure, which can clearly express the botanical characteristics of trees. In the process of model visualization, we hope to preserve the hierarchical structure features of trees as completely as possible to provide more detailed scene composition information for the construction of garden vegetation landscapes. Therefore, the parameterized tree model has a

large amount of data and high rendering consumption, the 3D landscape drawing module integrates the TreeEngine. The specific rendering process of realizing the loading and rendering of tree model into 3D scene is shown in Figure 3 [13].

The whole process of tree model loading and rendering based on TreeEngine can be divided into two processes. If the vegetation model loaded into the scene is judged to be parameterized model format (.pTM), OSG default model support format will be used for loading and rendering. In this way, the hierarchical optimization of the model is not carried out, and the overall loading and rendering effect of the model depends on the structural parameters of the model itself, if the format of the parameterized tree model loaded into the scene is judged to be yes, the tree structure will be rendered step by step in a hierarchical manner, and the branches of each level will be rendered and drawn independently to build a tree model flow chart with real morphological structure. TreeEngine in the process of tree visualization is a series of functions built to achieve parametric tree model rendering to OSG 3D scene [14, 15].

3.1.3. Landscape Architecture Construction. Buildings are an important part of the artificial landscape, and the study of rapid and universally applicable modeling methods for buildings is very important for the process of virtual reality scene construction. The rapid construction of 3D building models by simple methods does not require repeated measurement and reconstruction of common building models for field scenes but can be generated in batches by unified methods [16].

Through the digitalization of building plane vector map, the building vector layer in shape format is generated. Based on this layer, the properties of the building are parameterized, including the building height, building wall map index, building top map index, building attribute (applicable to special cases such as overhead floors), and so on. A series of parameterized attribute sets are taken as the parameter list of building elements, and the height attribute is taken as the stretch amount from the two-dimensional building appearance vector to the three-dimensional building model to pull the building up and generate the white model of the building. And through the mapping index, the architectural mapping data indexed by XML file can be mapped to the corresponding garden buildings one by one, forming a batch of buildings with realistic sense and fast generation. The specific building construction process is shown in Figure 4 [17, 18].

In the process, building elements are generated and building styles are set through the corresponding method in osgEarth toolkit. The building appearance and other attributes are symbolized, combined with the corresponding texture map index, to generate realistic buildings or group models in batches [19].

3.1.4. GLSL Workflow. Graphics processor (graphics processing unit, GPU) rendering triangles in accelerating technology is through its powerful computing power and

TABLE 1: Data table of tree morphological and structural parameters (a case study of goldenrod frangipani).

| Hierarchy	Branches number	Stem length	Panel length	Branch angle	Branches diameter
A central dry	0	0.48 m	0.48 m	None	0.24 m
	1-1	0.33 m	0.12 m	176°	0.18 m
The primary branches	1-2	0.40 m	0.13 m	159°	0.15 m
	1-3	0.35 m	0.11 m	161°	0.19 m
Secondary branches	2-1-1	0.51 m	0.34 m	137°	0.07 m
	2-1-2	0.45 m	0.27 m	164°	0.05 m
	2-1-3	0.47 m	0.27 m	134°	0.09 m
Level 3 branches*	. . .	. . .	. . .	. . .	. . .
Whether in whorls no		Leaf blade density38.4/m³ canopy1.73 m height of tree 2.26 m			
Yes no result no		Leaf position branch tip leaf cluster 6-8piece/cluster texture style bitmap			
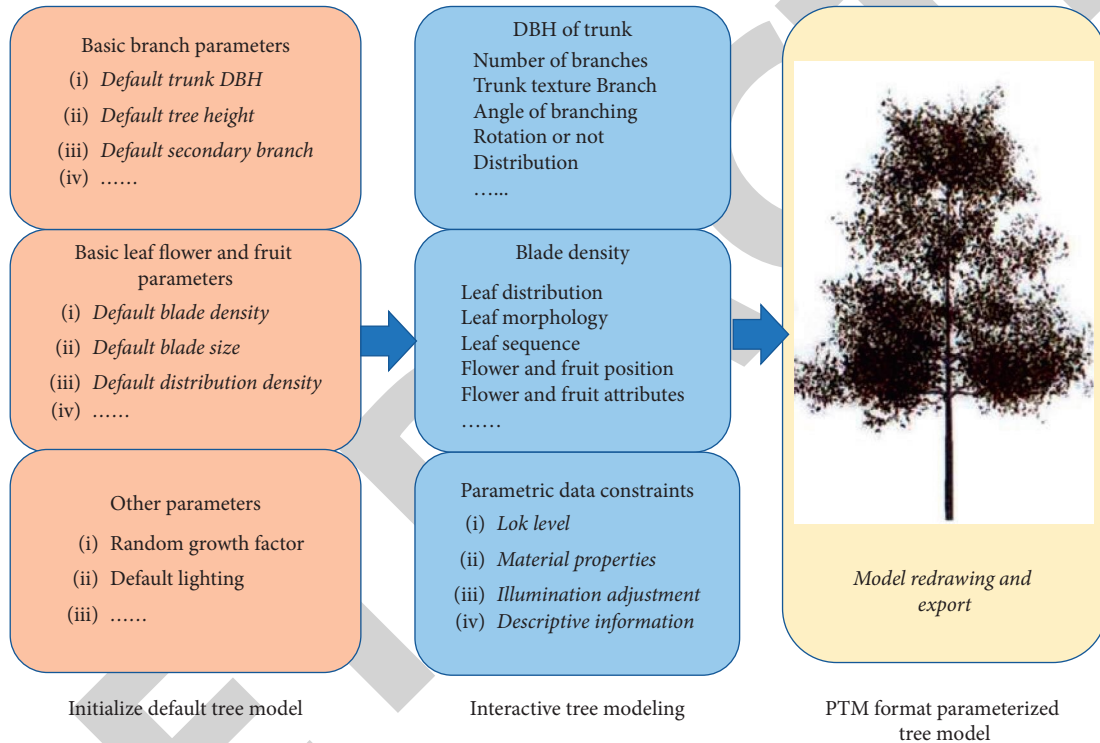
FIGURE 2: Parametric tree modeling process.

speed of floating point arithmetic, rest to handle complex 3D model another drawing, reduce the CPU in each frame 3D scene geometry in the process of drawing and processing workload. GLSL, namely, OpenGL shader language. In 3D scene rendering based on computer graphics rendering interface OpenGL, it is a high-order coloring language executed on GPU by defining program language instead of fixed drawing pipeline part function. In the OSG graphics rendering engine, support for GLSL is encapsulated in detail. The workflow of GLSL is gradually rendered from vertex shader to chip shader by using shader class Program to draw graphics of the overall 3D scene, as shown in Figure 5 [20].

The scene leaf vertex data is obtained by vertex shader, the corresponding raster processing is carried out, and transferred to the chip shader, which enters the GPU rendering pipeline and synchronizes CPU to render and draw a large number of tree leaves [21].

3.1.5. Tree Leaf GPU Accelerated Rendering Implementation. In the TreeEngine module, the Billboard function is provided in the OSG graphics rendering engine to simplify the processing of leaf data. By rendering the leaf geometry to the rectangular geometry of the corresponding viewpoint, the Billboard determines the viewpoint position in the 3D scene and performs synchronous rendering of the rectangular geometry. Similarly, we use GLSL in vertex shader to complete the matrix transformation of the scene viewpoints corresponding to the blade geometry so that the drawn blades face the line of sight direction synchronously, and achieve the function similar to Billboard. The difference is that these steps are executed synchronously on the GPU drawing pipeline, and the reduction of the number of GPU drawing calls directly improves the overall rendering efficiency of the program [22].
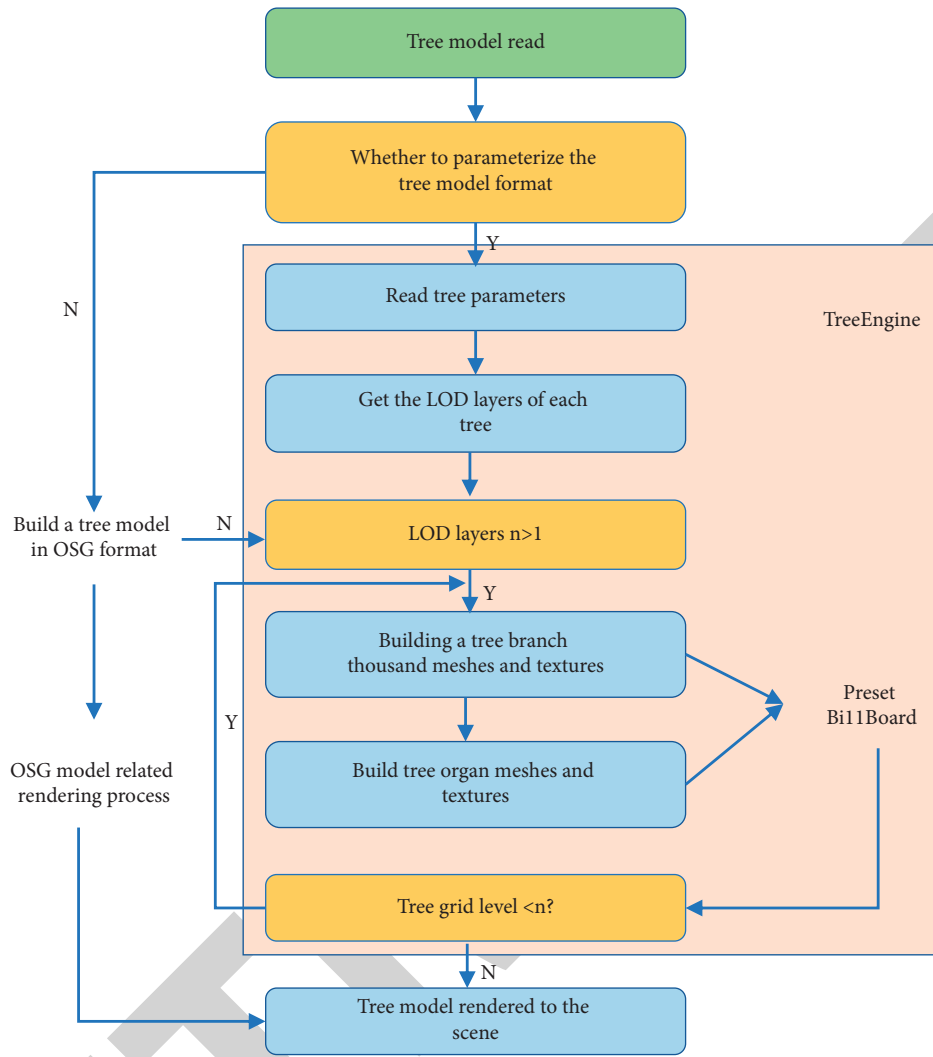
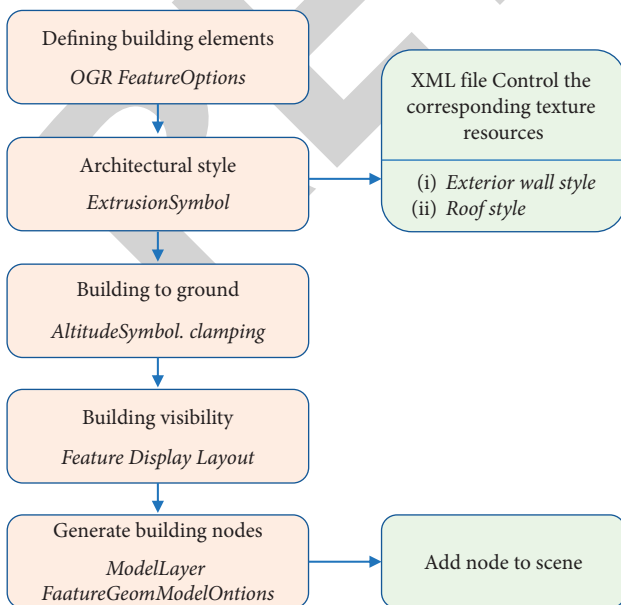FIGURE 3: Tree model value dyeing visualization process.
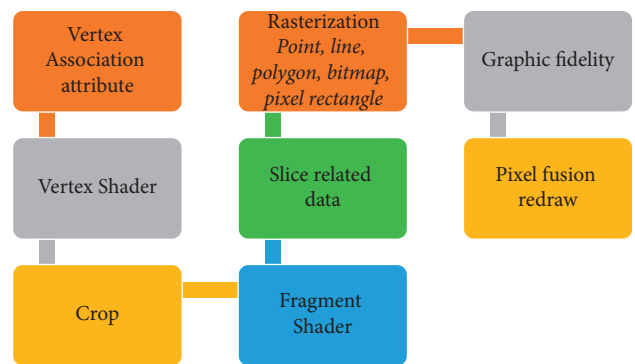

FIGURE 4: Building construction process.

FIGURE 5: Vertex shader and slice shader workflow.

Due to its hierarchical structure, the parameterized tree model can be processed in GLSL by grouping and caching according to the hierarchical organizational structure, and the hierarchical branch structure can be sequentially processed in THE GPU rendering pipeline. Because of its simple structure, the vertex shader only defines the vertex position

of each level of the branch, the index of the upper level of the branch, and the length of the branch, and draws the appearance of the branch through the transformation of the corresponding vertex data. In the slice shader, all levels of branch nodes with vertex positions are uniformly drawn, and the corresponding branch texture maps are specified to realize the rendering of realistic tree branches at all levels [23].

4. Ecological Land Model Design Based on Improved Genetic Algorithm

4.1. Overall Optimization Objective of the Model. The application of the NSGA-II algorithm in land allocation optimization is realized by the bionic logic of genetic evolution in the algorithm. From the perspective of process steps, land allocation structure needs to be converted into genotypes, and *X* randomly generated land allocation schemes are used as the initial population in the algorithm model. And use the method of choice, and a series of crossover and mutation operations to realize the generation of initial population optimization, out the individual relative inferiority, retain the optimization results, and according to the objective function to obtain a set of following the constraint condition of an optimal solution set of the solution set is ultimately retained within individual optimization to get the actual application of the optimized land use allocation plan. The specific process is as shown in Figure 6:

(1) In the coding part, the optimization problem is coded by real number coding method, in which the land type is coded as real number. Real number is the external phenotype of the algorithm and the mapping result of genotype in the algorithm logic. Real coding is to represent individual gene values with the help of real numbers. Through coding, any set of state schemes of quantitative structure of land use is expressed as a chromosome if there are *N* land use types in a land allocation optimization problem to be solved. Then, the number of genes on the chromosome in the genetic algorithm is *N*, and the genes on the chromosome refer to the ID of land use type, while the gene value on the chromosome represents the land area scale of different land use types.

In Figure 6, a plot of land use allocation optimization scheme is taken as an example: if there are *N* land use types in this study, then the number of genes on chromosomes is *N*, which is encoded by real numbers. Variable XI is a real number, representing the size of land use area of different land types, namely, the gene value on chromosomes.

(2) In the study of this kind of problem, population initialization means that *N* individuals are randomly generated in the initial population to represent *N* kinds of land use structure schemes, which are called *N* chromosomes in NSGA-II algorithm. The whole algorithm process starts from the initial population and the value of gene loci of
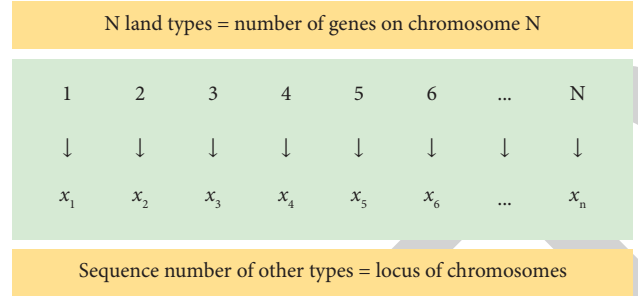

Figure 6: Application of NSGA-II algorithm in land allocation problem.

any individual in the initial population is obtained by the following formula:

$$x_i = d \times (\max(x_i) - \min(x_i)) + \min(x_i), \quad (1)$$

$$d = r\text{and}. \quad (2)$$

In formula (1) abovementioned, x_i is the area value of class I land use type, d is a random value with a value range of (0,1), and rand() is a random function.

(3) Fitness function, as the reference condition of the algorithm model for individual optimization in practical calculation, is the actual mapping of the judgment condition of survival of the fittest after natural selection in genetic evolution in the algorithm logic. In NSGA-II algorithm, the fitness of each individual is determined by non-dominant grade and crowding, rather than directly calculated according to the objective function. In addition, fitness is not a direct fitness value in the genetic algorithm, but a priority level calculated according to the non-dominant class and crowding degree. In the actual calculation process, the non-dominant rank of an individual is determined first. If the rank is higher, the individual will be selected for the next generation population to continue optimization calculation. If the individual is in the same rank, the representative with a larger crowding distance is relatively dispersed compared to its crowding degree and can be selected to continue optimization calculation.

The crowding degree can be obtained by calculating the sum of the distance between an individual and two neighboring individuals with the same level as the individual and each sub target. The calculation of crowding degree is related to the number of objective functions. If n objective functions are set in this quasi-optimization problem, the crowding distance of individual A can be calculated as follows:

$$a_h = \sum_{m=1}^{n} (f(a+1)_m - f(a-1)_m). \quad (3)$$

4.2. Algorithm Improvement in Optimization Model. The algorithm content of the research part of the urban

ecological land optimization model proposed in this study is mainly realized based on the improved NSGA-II algorithm. Compared with the classical ALGORITHM of NSGA-II, the difference lies in the transformation of the acquisition method of variation operator and scaling factor.

4.2.1. Mutation Operator Optimization Part. For genetic optimization algorithm, the mutation operation is an essential part of its three operations. In mutation operations, is the most important target is the optimization of mutation operator, this is due to the design of the mutation operator will be a larger extent, the operating efficiency of the implementation of algorithm, and the convergence of the algorithm in the optimization process of great influence.

In order to improve the defect of NSGA-II algorithm in the problem of population diversity, it is necessary to optimize and design the variation operator used in the classic NSGA-II algorithm. The variation operator used in this algorithm is polynomial variation operator, which has strong subjectivity and requires the decision maker to set the polynomial variation operator subjectively and can generally be expressed as:

$$x_{ij}(t) = x_{ij}(t) + \Delta_j. \tag{4}$$

The manner of obtaining Δ_j is:

$$\Delta_j = \begin{cases} (2\beta)^{1/\gamma+1} - 1, \beta \le 0.5, \\ (1 - (2(1-\beta)))^{-1/\gamma+1}, \beta > 0.5. \end{cases} \tag{5}$$

In view of the deficiency of polynomial mutation operator, the idea of differential evolution algorithm is brought into NSGA-II algorithm in this study, and the mutation operator in NSGA-II algorithm is designed and optimized. Differential evolution (DE) algorithm, as an algorithm for real number optimization problems, is an adaptive global optimization algorithm based on population. It has the advantages of concise structure, easy implementation, rapid convergence, and a strong algorithm. With the artificial intelligence in recent years and the rise of big data technology and development, this kind of algorithm in data mining, pattern recognition, and artificial neural network, and other aspects have a relatively strong performance of DE algorithm and genetic algorithm, are depending on different individuals in the group cooperation and competition to search heuristic optimization solution behavior direction is the basic logic of DE algorithm:

(1) Generate an initial population randomly, pair the individuals in the population in pairs, calculate the vector difference of any pair of individuals, and sum it with the third individual to obtain a new individual;

(2) The fitness of the new individuals obtained is compared with that of the corresponding individuals in the contemporary population. If the new individuals obtained have good performance in fitness, the current individuals are eliminated and the new individuals are selected to complete optimization

and enter the next generation population for further optimization operations; otherwise, the current individuals are retained and enter the next generation population. Through this logic, the population can be evolved many times, so as to realize the preservation of excellent individuals and the proposal of inferior individuals, and finally tend to the emergence of the optimal solution set.

In this process, the different strategy has outstanding performance. In general, what this strategy implement is to randomly acquire a pair of individuals in the contemporary population, perform vector difference scaling operation on them, and combine the operation result with the individuals to be mutated, which can be expressed as:

$$C_i(g+1) = X_{ri}(g) + F \cdot (X_{r2}(g) - X_{r3}(g)). \tag{6}$$

Represented by the formula (6), F is a scaling factor, while $x_i(g)$ moving refers to the first generation of g populations in the case of an individual I. In addition, the effectiveness of the solution is usually achieved through determining chromosomes gene in marginal conditions to ensure that, if the gene can't meet the requirements of marginal conditions, may need to be done in accordance with the initial population access way to random to regenerate. It can be expressed as:

g population:

$$\left\{ X_i(g) | X_{j,i}^L \le X_{j,i}(g) \le X_{j,i}^U, i = 1, 2, \ldots, NP; j = 1, 2, \ldots, D \right\}. \tag{7}$$

After the mutation operation, an intermediate is formed:

$$\begin{aligned} \{ C_i(g+1) | C_{j,i}^L \le C_{j,i}(g+1) \le C_{j,i}^U, \\ i = 1, 2, \ldots, NP; j = 1, 2, \ldots, D \}. \end{aligned} \tag{8}$$

As can be seen from the abovementioned, DE algorithm is a global optimization algorithm based on population initialization. In fact, DE algorithm itself also has the idea of preservation. Its unique differential variation strategy can affect the direction trend of individual evolution in the population during optimization and disturb it:

$$C_i^n = X_{r1}^n + F \cdot (X_{r2}^n - X_{r3}^n). \tag{9}$$

The difference variation method is introduced into NSGA and an important aspect of the algorithm is to transform the formula of the standard difference algorithm into the iterative optimization structure of NSGA-II algorithm. The transformation process can be expressed as formula (10):

$$C_i^{n+1} = X_{r1}^n + F_1 \cdot (X_b^n - X_i^n) + F_2 \cdot (X_{r1}^n - X_{r2}^n). \tag{10}$$

As the optimal individual that can be selected, the acquisition quality of X_b^n will greatly affect the optimization process and results, and how to obtain it is actually an important step in the implementation of differential variation strategy in NSGA-II algorithm. Because this research is oriented to the multi-objective land allocation optimization problem, and the multi-objective problem has multiple X_b^n

objective functions, how to select the appropriate X_b^n is more important. In order to solve this problem, in the implementation of differential variation operation, according to the non-dominated sorting mechanism naturally possessed by NSGA-II algorithm, the operation of dominance relation is combined with the implementation of DE method. The mathematical expression of dominance relation is as follows:

$$
C_i^{n+1} = \begin{cases} C_{1i}^{n+1}, & C_i^{n+1} \succ C_{2i}^{n+1}, \\ C_{2i}^{n+1}, & \text{軑}, \end{cases}
$$
$$
C_i^{n+1} = \left(C_{1i}^{n+1}, C_{2i}^{n+1}, \ldots, C_{ki}^{n+1} \right), k = 1, 2, \ldots, m. \tag{11}
$$

In general, the differential evolution strategy is actually to inspire the algorithm to search the spatial region where the optimal solution is based on the differences of different individuals in the same population. In the early stage of the search, the non-dominant solution set in the population should be obtained, and the adjacent individuals to be searched locally should be set as the parent individuals, and then the offspring individuals can be obtained through the calculation of the difference formula. The current non-dominant solution set individual is determined by comparing the non-dominant relationship between the father and the son. If they are in the non-dominant relationship, the offspring will be added to the non-dominant solution set. If they are not in the non-dominant solution set, they will be removed. After the operation logic, the superior individuals in the non-dominant solution are selected based on the comparison method of crowding.

4.2.2. Scaling Factor Optimization Part. The transformation of NSGA-II algorithm based on differential variation strategy involves a relatively important variable factor, namely, scaling factors F_1 and F_2. In the classical differential evolution method, these two factors are usually set by the decision maker in the process of decision making. In the traditional NSGA-II algorithm, its algorithm mechanism leads to unsatisfactory optimization convergence efficiency. Therefore, how to achieve balanced performance and efficiency improvement in the multi-objective optimization problem scenario in algorithm transformation is a problem related to the optimization process and results.

The objective of this optimization is to give consideration to the performance and efficiency of scaling factors F_1 and F_2, which can be understood as the following two aspects when applied to the multi-objective optimization problem represented in this study: In the early optimization process to improve the efficiency of the search process, can quickly complete the overall search; In the middle and second half, the ability of local search is strengthened, as shown in Figure 7.

Through the related elaboration and expression of differential evolution strategy, it can be concluded that the value of F tends to shrink with the continuous expansion of the current evolution algebra, but the value of F has a very direct and important influence on the optimization efficiency of the algorithm optimization process. Based on the above understanding, we can know that the optimization

speed of the algorithm is actually gradually from fast to slow with the increase of the current evolutionary algebra. However, the difference is that in the process of the gradual increase of the current evolutionary algebra, the value of F_2 is gradually increased with the evolutionary algebra, and the value of F_2 is directly related to the local convergence ability of the algorithm in the middle and later stage of optimization. Based on the goal shown in Figure 7, the scaling factor needs to be modified so that it can be adjusted in real time. Here the adjustment mechanism is optimized based on linear algebra.

$$
F_1 = F_{\max} - \frac{n(F_{\max} + F_{\min})}{N},
$$
$$
F_2 = F_{\max} - \frac{n(F_{\max} + F_{\min})}{N}. \tag{12}
$$

In the above formula, $F_{\max}$ and $F_{\min}$ represent the maximum and minimum values of the scaling factor, and their values are between 0 and 1. The optimization efficiency in the whole process of the algorithm can be taken into account by linear real-time adjustment of steam and fan scaling factors.

4.2.3. Actual Algorithm Flow. The optimized algorithm flow is shown in Figure 8, which is detailed as follows:

(1) Initialize the population to obtain an initial population, and select parameters according to the actual problem scenario;

(2) Through the method of championship, several individuals were selected into the hybrid pool, and the individuals in the pool were binary crossover and differential variation, and then the new individuals were obtained;

(3) After the population generation, the parent and child populations were merged, and a fast non-dominated sequence was carried out for the combined new population, and the non-inferior frontier was determined;

(4) The non-inferior front obtained in the previous step was sorted according to the crowding distance calculation, and the sorted individuals were optimized to obtain the new population;

(5) Determine whether the termination condition of the cycle is triggered or whether the evolution algebra reaches the maximum. If it is determined to be yes, the algorithm process will be ended; if it is determined to be no, the second step will be returned to continue the cycle operation.

In terms of the time complexity of the algorithm, the time complexity of the optimized NSGA-II algorithm has changed the mutation operation strategy. However, time complexity still remains $O(MN^2)$, where M and N refer to the number of objective functions and population size respectively. It can be seen that there is no change in time complexity.
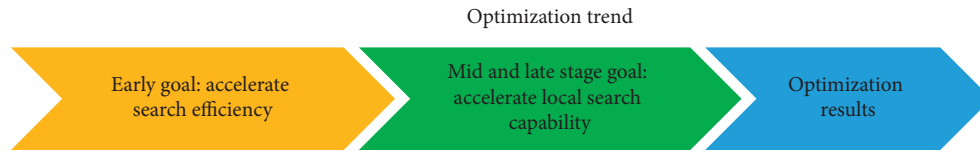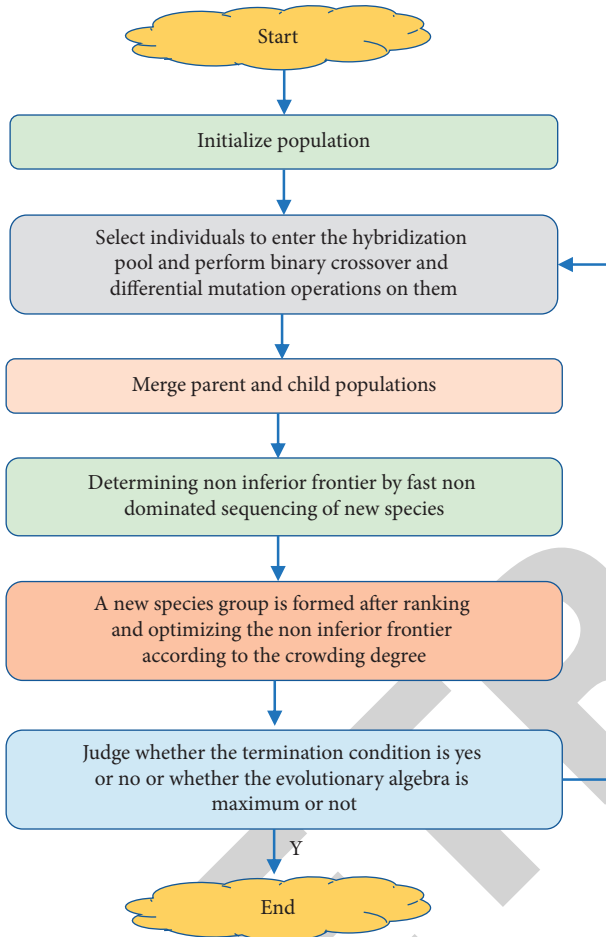
FIGURE 7: Optimization objective.

FIGURE 8: Algorithm flow chart.

4.3. Experimental Analysis. In order to compare the efficiency of the two different rendering optimization methods, we constructed a forest scene on a simple terrain, and 144 identical trees were generated on the terrain with rows and rows of 3 meters apart. The whole scene did not include other elements to eliminate other influencing factors.

According to the location of the camera node, the scene geometry information of each viewpoint was counted. As the main basis for comparative analysis, the following data were mainly based on Table 2. The total number of graphable geometric triangles and vertices of scenes from each viewpoint were counted respectively.

According to the data in Table 2, it is obvious that the smaller the visual distance is, the smaller the amount of scene drawing data is, mainly because the clipping scope of the visual cone is different in different visual fields. The

smaller the visual distance is, the less scene content will enter the visual field of the visual cone.

The running frame rate (FPS) of the forest scene under the four viewpoints is obtained, and the rendering efficiency of different rendering methods can be intuitively reflected through comparative analysis. In order to facilitate comparison, the program frame rate was obtained every 3 seconds for 25 times (75 seconds). The specific frame rate was obtained from the osgUtil: statistics state set of the OSG graphics rendering engine.

Based on different viewing distances, viewpoints 1 and 2 were taken as scenes with large data volumes, while viewpoints 3 and 4 were taken as scenes with small data volumes for an independent analysis. The results are shown in Figure 9.

According to the results of Figure 9, in the case of viewpoint 1 and Viewpoint 2 with a large amount of scene data, the rendering frame rate of the overall scene fluctuates around 4 frames per second, and the rendering effect of the scene is not ideal. Correspondingly, although the frame rate of scenes drawn by GPU accelerated rendering method has slight improvement, it still cannot meet the minimum requirement of real-time rendering of 3D scenes, namely, 30 frames per second. Therefore, the conclusion can be drawn: when the total amount of data in the scenario is large, GPU accelerated rendering method based on GLSL method cannot meet the real-time rendering requirements of 3D landscape. It is limited by hardware device performance and needs to consider many factors.

As a comparison, the rendering results of viewpoint 3 and viewpoint 4 with less rendering volume are significantly different. When the amount of scene data is small, the comparison of the two rendering methods is shown in Figure 10.

In Figure 10, under the premise of an acceptable amount of data, the rendering frame rate of the forest scene is better, which increases from 35–42 frames per second of the traditional OSG rendering method to about 60 frames per second. The average render rate increased by about 30%, and the scene's maximum renders speed of 60 frames per second was largely due to the maximum refresh rate of the desktop hardware display screen. In the virtual reality headset display equipment, the lens display of the equipment has a higher refresh rate, so the scope of view of the user's first angle view is smaller. The application of GPU accelerated rendering method based on GLSL method can significantly improve the rendering efficiency of 3D landscape scenes with a large number of trees and vegetation. Therefore, the application of GLSL programming method and the use of GPU acceleration to draw a tree model with a large number of faces can

Table 2: The geometric graph information statistics of the four test viewpoints.

Point number	Range of visibility (m)	Body that can be drawn	Geometry	He triangle	Climax
Viewpoint 1	200	11968	370	0416	305168
Viewpoint 2	200	11303	373	3490	302699
Viewpoint 3	100	6644	180	0276	213841
Viewpoint 4	100	5826	171	1186	207398

- Viewpoint 1 Accelerated rendering
- Viewpoint 2 Accelerated rendering
- Viewpoint 1 General rendering
- Viewpoint 2 General rendering
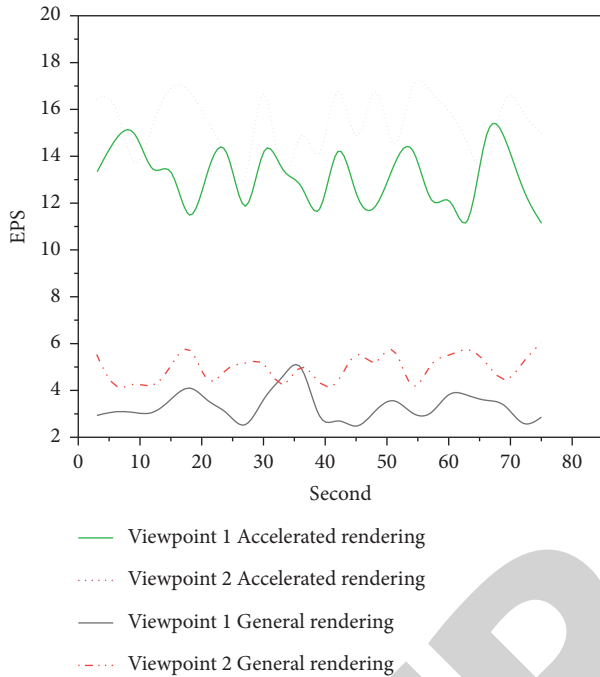
Figure 9: Frame rate comparison between viewpoint 1 and viewpoint 2.

- Viewpoint 3 Accelerated rendering
- Viewpoint 4 Accelerated rendering
- Viewpoint 3 General rendering
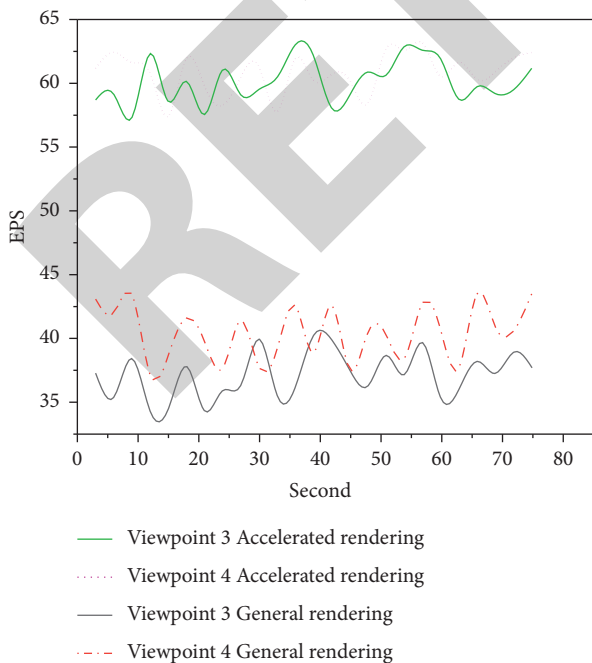- Viewpoint 4 General rendering

Figure 10: Frame rate comparison between viewpoint 3 and viewpoint 4.

effectively improve the rendering efficiency of 3D scenes under the condition of small user visual distance and a small amount of visual body clipping operation, which provides help for immersive virtual reality display to a certain extent.

5. Conclusion

Based on the construction of a visualization model base on urban ecological landscape plants, the batch visualization of urban ecological landscape plants was studied. After summarizing and describing the main research methods of plant visual model bank, a set of species selection logic and method of urban ecological landscape plant model bank was proposed. In addition, a set of logical methods and processes for the construction of an ecological plant visual model base were designed and an optimization scheme of plant model was proposed to balance the realism and rendering efficiency of the model base.

Based on the parametric method to construct 3D landscape scenes, the main elements of the landscape were, respectively, constructed and rendered 3D models. It includes parameterized 3D tree model, 3D terrain landscape real-time fluctuating water body based on UAV point cloud data, various garden building models, etc. All kinds of landscapes are visualized under the OSG graphics rendering engine. Through the spatial organization of parametric vector control, a complete 3D landscape scene construction process is formed. Aiming at the real-time demand of 3D scenes, the study of GPU accelerated rendering and rendering of vegetation leaf surface data based on GLSL were carried out. The unified rendering of leaves was realized by OpenGL shader language, and the unified orientation matrix calculation was carried out for the surface data. It stimulates the Billboard function of the OSG graphics rendering engine to reduce the number of GPU calls and improve the rendering efficiency of landscape vegetation. The different vegetation rendering methods are compared and analyzed. The experimental results show that the GPU accelerated rendering method based on GLSL can significantly improve the frame rate of rendering 3D landscape vegetation scenes with a small amount of scene data, which has certain feasibility.

Data Availability

The dataset can be accessed upon request.

Conflicts of Interest

The authors declare that they have no conflicts of interest.

References

[1] L. I. Guoqing, J. Zhu, and W. U. Guohua, "Ecological landscape planning and design of zhuxi river in chongqing," *Asian Agricultural Research*, vol. 12, no. 6, p. 4, 2020.

[2] J. Langreck, H. Wong, A. Hernandez et al., "Modeling and simulation of future capabilities with an automated computer-aided wargame," *The Journal of Defense Modeling and Simulation: Applications, Methodology, Technology*, vol. 18, no. 4, pp. 407–416, 2021.

[3] J. Yuan, H. Abdul-Rashid, B. Li et al., "A comparison of methods for 3d scene shape retrieval," *Computer Vision and Image Understanding*, vol. 201, no. 4, Article ID 103070, 2020.

[4] X. Zhao, "Application of 3d cad in landscape architecture design and optimization of hierarchical details," *Computer-Aided Design and Applications*, vol. 18, no. S1, pp. 120–132, 2020.

[5] T. S. Bailey and S. Alva, "Landscape of continuous glucose monitoring (cgm) and integrated cgm: accuracy considerations," *Diabetes Technology & Therapeutics*, vol. 23, no. S3, pp. S-5–S-11, 2021.

[6] C. L. Zimmer, E. von Seth, M. Buggert et al., "A biliary immune landscape map of primary sclerosing cholangitis reveals a dominant network of neutrophils and tissue-resident t cells," *Science Translational Medicine*, vol. 13, no. 599, Article ID eabb3107, 2021.

[7] G. Y. Xie, C. J. Liu, Y. R. Miao, M. Xia, Q. Zhang, and A. Y. Guo, "A comprehensive platelet expression atlas (pea) resource and platelet transcriptome landscape," *American Journal of Hematology*, vol. 97, no. 1, pp. E18–E21, 2022.

[8] J. Huang and X. Zhou, "Interactive application of vr technology in ice and snow landscape design," *Journal of Physics: Conference Series*, vol. 1744, no. 3, Article ID 032100, 2021.

[9] D. Wang, X. Ji, C. Li, and Y. Gong, "Spatiotemporal variations of landscape ecological risks in a resource-based city under transformation," *Sustainability*, vol. 13, no. 9, p. 5297, 2021.

[10] M. Ronse, J. Irani, C. Gryseels et al., "In pursuit of a cure: the plural therapeutic landscape of onchocerciasis-associated epilepsy in Cameroon – a mixed methods study," *PLoS Neglected Tropical Diseases*, vol. 15, no. 2, Article ID e0009206, 2021.

[11] S. C. Bohra and J. Purkayastha, "An insight into the butterfly (lepidoptera) diversity of an urban landscape: guwahati, Assam, India," *Journal of Threatened Taxa*, vol. 13, no. 2, pp. 17741–17752, 2021.

[12] T. Zachrisson, "The queen of the mist and the lord of the mountain: oral traditions of the landscape and monuments in the omberg area of western östergötland," *Current Swedish Archaeology*, vol. 11, no. 1, pp. 119–138, 2021.

[13] G. B. Brandani, C. Tan, and S. Takada, "The kinetic landscape of nucleosome assembly: a coarse-grained molecular dynamics study," *PLoS Computational Biology*, vol. 17, no. 7, Article ID e1009253, 2021.

[14] A. Dechaicha, A. Daikh, and D. Alkama, "Monitoring and landscape quantification of uncontrolled urbanisation in oasis regions: the case of adrar city in Algeria," *Journal of Contemporary Urban Affairs (JCUA)*, vol. 5, no. 2, pp. 209–219, 2021.

[15] G. Li, F. Liu, A. Sharma et al., "Research on the natural language recognition method based on cluster analysis using neural network," *Mathematical Problems in Engineering*, vol. 2021, Article ID 9982305, 13 pages, 2021.

[16] D. Selva, B. Nagaraj, D. Pelusi, R. Arunkumar, and A. Nair, "Intelligent network intrusion prevention feature collection and classification algorithms," *Algorithms*, vol. 14, no. 8, p. 224, 2021.

[17] J. Chen, J. Liu, X. Liu, X. Xu, and F. Zhong, "Decomposition of toluene with a combined plasma photolysis (cpp) reactor: influence of uv irradiation and byproduct analysis," *Plasma Chemistry and Plasma Processing*, vol. 41, no. 1, pp. 409–420, 2020.

[18] R. Huang, S. Zhang, W. Zhang, and X. Yang, "Progress of zinc oxide-based nanocomposites in the textile industry," *IET Collaborative Intelligent Manufacturing*, vol. 3, no. 3, pp. 281–289, 2021.

[19] M. K. A. Kaabar, V. Kalvandi, N. Eghbali, M. E. Samei, Z. Siri, and F. Martínez, "A generalized ML-hyers-ulam stability of quadratic fractional integral equation," *Nonlinear Engineering*, vol. 10, no. 1, pp. 414–427, 2021.

[20] Y. Xia, "The influence of artificial intelligence on the diversity of plant design in landscape design," *Journal of Physics: Conference Series*, vol. 1744, no. 2, Article ID 022104, 2021.

[21] S. T. G. Lim and F. Perono Cacciafoco, "Discovering unwritten stories: a modular case study in promoting landscape education," *Education Sciences*, vol. 11, no. 2, pp. 68–16, 2021.

[22] B. H. Goodge, D. Li, K. Lee et al., "Doping evolution of the mott–hubbard landscape in infinite-layer nickelates," *Proceedings of the National Academy of Sciences of the United States of America*, vol. 118, no. 2, Article ID e2007683118, 2021.

[23] X. Guan, H. Zhu, J. Zhang et al., "Landscape of idh mutations in patients with solid tumors: a pan-cancer analysis," *Journal of Clinical Oncology*, vol. 38, no. 15, Article ID e13638, 2020.